Journal of Hepatocellular Carcinoma

Dovepress
open access to scientific and medical research

Open Access Full Text Article

ORIGINAL RESEARCH

Estimating Microvascular Invasion in Patients with Resectable Multinodular Hepatocellular Carcinoma by Using Preoperative Contrast-Enhanced MRI: Establishment and Validation of a Risk Score

Fei Wu[1,2,*], Haitao Sun[1,2,*], Zhang Shi[1,2], Changwu Zhou[1–3], Peng Huang[1,2], Yuyao Xiao[1,2], Chun Yang[1,2], Mengsu Zeng[1–3]

[1]Department of Radiology, Zhongshan Hospital, Fudan University, Shanghai, People's Republic of China; [2]Department of Cancer Center, Zhongshan Hospital, Fudan University, Shanghai, People's Republic of China; [3]Shanghai Institute of Medical Imaging, Zhongshan Hospital, Fudan University, Shanghai, People's Republic of China

*These authors contributed equally to this work

Correspondence: Mengsu Zeng, Department of Radiology, Zhongshan Hospital, Fudan University; Shanghai Institute of Medical Imaging, No. 180 Fenglin Road, Xuhui District, Shanghai, 200032, People's Republic of China, Tel +86 13501922963, Email zeng.mengsu@zs-hospital.sh.cn; Chun Yang, Department of Radiology, Zhongshan Hospital, Fudan University, No. 180 Fenglin Road, Xuhui District, Shanghai, 200032, People's Republic of China, Tel +86 18702135336, Email dryangchun@hotmail.com

Objective: To determine the preoperative clinicoradiological factors to predict microvascular invasion (MVI) in patients with resectable multinodular hepatocellular carcinoma (mHCC), and further to establish and validate a stratified risk scoring system.

Methods: Two hundred and seventy-three patients with pathologically confirmed mHCC (≥2 lesions) without major vascular invasion and biliary tract tumor thrombosis, who underwent preoperative contrast-enhanced MRI and hepatectomy, were consecutively enrolled (training/validation cohort=193/80). Preoperative clinicoradiological variables were collected and analyzed. The multivariable logistic regression was performed to determine the independent predictors of MVI and create a risk score system. The C-index, calibration curve and decision curve were used to evaluate the performance of the risk score. A risk score-based prognostic stratification system was performed in mHCC patients. The risk score system was further verified in the validation cohort.

Results: AFP > 400 ng/mL, presence of satellite nodule, mosaic architecture and increased total tumor diameter were independent predictors of MVI while fat in mass was an independent protective factor of MVI. The risk score yielded satisfactory C-index values (training/validation cohort: 0.777/0.758) and fitted well in calibration curves. Decision curve analysis further confirmed its clinical utility. Based on the risk score, mHCC patients were stratified into high-/low-MVI-risk subgroups with significantly different recurrence-free survival (both $P < 0.001$).

Conclusion: The presented risk score incorporating clinicoradiological parameters could stratify mHCC patients into high-risk and low-risk subgroups and predict prognosis in patients with resectable mHCC.

Keywords: hepatocellular carcinoma, prognosis, magnetic resonance imaging, statistical model

Introduction

Hepatocellular carcinoma (HCC) often manifests with multiple tumors within the liver. About 50–75% of patients were initially diagnosed with multinodular HCC (mHCC), which was at the intermediate-to-advanced stage and posed a great challenge for the clinical management.[1–3] Compared with single-nodular HCC, mHCC is characterized with intertumoral heterogeneity in terms of biological behavior, leading to a great variability in optimal treatment. The current Barcelona Clinic Liver Cancer guideline recommends different treatment options for patients with mHCC at different stages. In specific, patients with mHCC at early stage are recommended radical surgery including liver resection and

Received: 21 March 2023
Accepted: 7 July 2023
Published: 20 July 2023

transplantation, while those with intermediate-to-advanced-stage mHCC are recommended nonsurgical treatments, such as transarterial chemoembolization or systemic therapies.[4] Liver resection has recently been gradually admissive for selected patients with mHCC when their preoperative liver function is tolerable and postoperative residual liver is expected to function well.[5] More studies have proven that liver resection provides a better survival benefit, broadening resection criteria for intermediate-to-advanced-stage mHCC patients.[5–8]

For patients with resectable mHCC, though surgical resection provides a potentially curative opportunity, the high postoperative recurrence rate remains a problem.[9,10] One of the major reasons is the presence of microvascular invasion (MVI).[11] MVI, known as microvascular cancer embolus, refers to the cancer cell nest in vessels lined with endothelial cells.[12] As an aggressive feature of HCC, it is the key factor related to early tumor recurrence, which decreased overall survival after resection.[12,13] For patients with mHCC, the incidence of MVI is even higher, as the multifocality may result from intrahepatic metastasis of the main tumor via MVI.[14,15] Considering its great impact on postoperative prognosis, estimating the status of MVI in patients with resectable mHCC before surgery may help to select those who would most benefit from surgical resection. However, information about MVI comes from postoperative specimens, which limits its utility in clinical practice. An accurate prediction of MVI with a noninvasive method is still challenging in mHCC patients.

A few efforts have been made on the preoperative estimation of MVI in mHCC. Previously, Zhao et al reported clinical parameters such as serum α-fetoprotein (AFP), γ-glutamyltranspetidase and total tumor diameter (TTD) were predictors of MVI in mHCC.[16] In addition to clinical variables, contrast-enhanced magnetic resonance imaging (MRI) could provide valuable information for the prediction of MVI as well. MRI features such as nonsmooth tumor margin, arterial peritumoral enhancement and incomplete radiological capsule were reported to be independent risk factors of MVI.[14,17–20] However, most of these studies were conducted in patients with solitary HCC and very few studies have focused on the prediction of MRI for MVI in patients with mHCC.

Recently, a risk scoring system has been reported as a novel and effective prediction model commonly used clinically.[21,22] Based on the total score, it generates the risk of MVI in patients with resectable mHCC, allowing a simple risk stratification. However, it has not been widely applied to predict MVI in patients with resectable mHCC. Therefore, in this study, we aimed to identify the preoperative clinicoradiological factors for predicting MVI in patients with resectable mHCC, and further to establish and validate a risk score-based prognostic stratification system.

Materials and Methods

The ethics committee of Zhongshan Hospital Fudan University approved this retrospective study (B2021-682R), which followed the Declaration of Helsinki's ethical guidelines. Written informed consent was waived due to its retrospective nature. We stated that patient data was strictly confidential.

Patients

We retrospectively and consecutively registered patients suspected of mHCC (≥2 HCC lesions) according to MRI reports from January 2015 to December 2018 by searching the electronic imaging database of the local institution. The lesion with satellite nodule, which was defined as a smaller nodule attached to or within 2 cm of the main tumor, was considered as one HCC lesion.[23]

Inclusion criteria were as follows: Patients with radical resection as the first-line treatment (R0 resection) and patients without major vascular invasion and biliary tract tumor thrombosis on preoperative MRI. The exclusion criteria were as follows: a) With a history of antitumor before surgery; b) Any lesion pathologically diagnosed as non-HCC after surgery; c) The presence of other malignant tumors; d) Insufficient MR image quality due to motion artifacts; e) Time interval between MR scan and surgery >1 month. A flowchart of inclusion and exclusion criteria is shown in Figure 1. The final cohort was split into two cohorts for training and validation at a ratio of 7:3 according to the data of the MR examination.

Laboratory Tests and Pathology

All clinicopathological information was documented from the medical records. The preoperative laboratory data included liver function, AFP levels, status of Hepatitis B or C virus infection and HBV deoxyribonucleic acid (HBV-DNA) load.

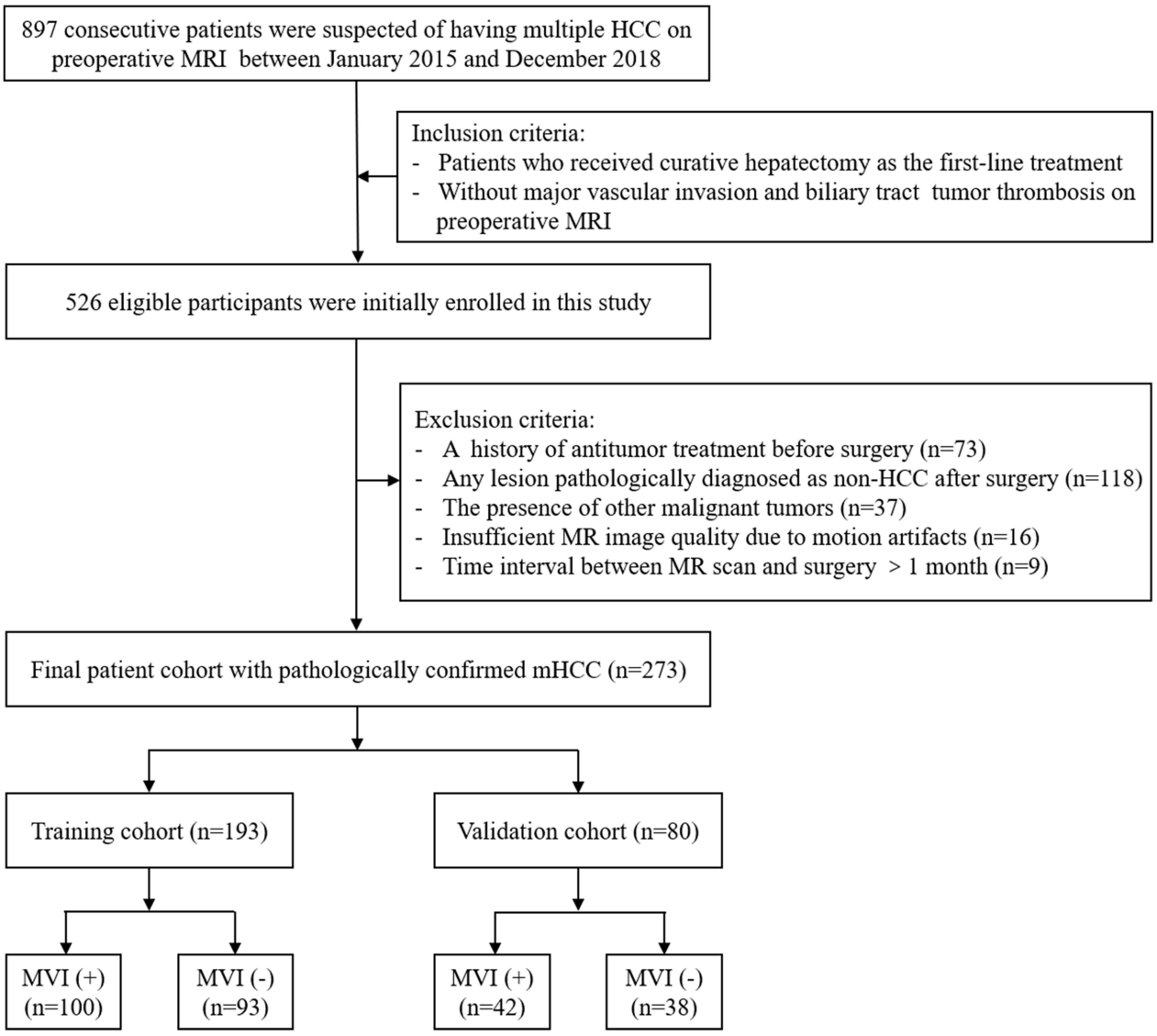

Figure 1 The flow chart of participants' inclusion and exclusion.
Abbreviation: MVI, Microvascular Invasion.

Pathological characteristics were assessed in consensus by 2 experienced pathologists (with 13 and 19 years of experience). MVI was defined as the presence of tumor emboli in the tiny blood vessels in the vicinity of any tumor.[24] Other features such as Edmondson-Steiner grade, satellite nodule and cirrhosis of the noncancerous liver parenchyma were also evaluated.

MR Imaging

All participants were examined on a 1.5 T MR scanner (MAGNETOM Aera, Siemens Healthcare) with a phased-array body coil. Unenhanced liver protocols are as follows: T1-, T2-, diffusion-weighted imaging and in/out-phase sequences. Afterward, the dynamic contrast-enhanced MR imaging was acquired with the contrast agent (gadolinium diethylenetriamine pentaacetic acid; Magnevist, Bayer HealthCare) administered at a dose of 0.1 mmol/kg at a flow rate of 2 mL/s. When contrast agent arrived at the ascending aorta using bolus, arterial phase acquisition was triggered, followed by the portal venous phase at 70–90 s and delayed phase at 160–180 s. The scanning parameter was shown in Supplementary Table 1.

MR Features Evaluation

Two radiologists (F.W. and H.T.S., with 7 and 12 years of experience) blinded to clinicopathological data independently evaluated the following qualitative MRI features: a) tumor number; b) tumor diameter; c) satellite nodule; d) hemorrhage in mass; e) fat in mass; f) arterial rim enhancement; g) radiological capsule; h) arterial peritumoral enhancement; i) mosaic architecture; j) nodule-in-nodule architecture; k) atypical enhancement pattern; l) radiological liver cirrhosis. If any tumor showed the image feature above, this feature was considered present in the patient. The definitions of these MRI features are described in Supplementary Material 1. If there was any disagreement between the two radiologists, a consensus was made with a third radiologist (C.Y., with 19 years of experience). Quantitative analysis was performed by the two radiologists as well, and the averaged values were used for further analysis. The largest tumor diameter (LTD), TTD and the ratio of the largest to the smallest tumor diameter (RLSD = diameter of the largest tumor/diameter of the smallest tumor) were calculated and documented.

Follow-Up

All participants were postoperatively followed up using serum AFP, liver function tests and imaging examinations of the chest and abdomen. During the first 2 years, these examinations were conducted once every 3 months and then once every 6 months thereafter. Tumor recurrence was defined as new intrahepatic and/or extrahepatic lesions diagnosed by CT/MRI, or confirmed by pathology. The data were censored on December 31, 2021. Recurrence-free survival (RFS) was defined as the interval from surgery to the first recurrence, metastasis, or last follow-up.

Statistical Analysis

χ^2 test or Fisher's exact test was used for categorical variables, and Student's test or the Mann–Whitney *U*-test was used for continuous variables.

Univariable and multivariable logistic regression analyses were performed to determine the independent predictors of MVI. The variables with $P < 0.10$ were entered into the multivariable logistic regression via backward stepwise selection. The multicollinearity was assessed using variation inflation factor with a threshold of 10. After determining the potential predictors of MVI in the training cohort, a simple risk score was developed. The detailed process was shown in the Supplementary Material 2. Based on the cut-off values of risk score, which was determined based on the best specificity, the cohort was divided into two risk groups, the high-risk group and the low-risk group. The RFS rates were estimated using the Kaplan–Meier method and differences between the high/low-risk groups were compared by the Log rank test. To evaluate inter-reader agreement, the Cohen's kappa was used for categorical variables and intraclass correlation for continuous variables.

SPSS software (version 22.0, IBM, Chicago, IL, USA) and R software (version 4.2.0, R project for Statistical Computing, Boston, MA, USA) were used for all statistical analyses. $P < 0.05$ was considered statistically significant.

Results

Baseline Characteristics

Initially, 526 eligible patients were included. After the exclusion, 273 pathologically confirmed mHCC patients were finally enrolled in the study. They were split into the training cohort (n = 193; MVI-positive/MVI-negative:100/93; men/women: 170/23) and validation cohort (n = 80; MVI-positive/MVI-negative: 42/38; men/women: 76/4). The total lesion number was 658 and the average number per patient was 2.4. The median follow-up time was 23.0 months (95% CI, 8.0–48.0). In the whole cohort, mHCC patients with histological MVI showed significantly decreased RFS than those without MVI ($P = 0.005$) (Supplementary Figure 1). The 1-year and 2-year RFS rates were 57.7%, 38.3% in patients with MVI-positive and 74.0%, 56.5% in patients with MVI-negative.

Table 1 summarizes the baseline characteristics of the two cohorts. No statistically significant difference was observed in the clinicopathological variables as well as the status of MVI between the training and validation cohort (all $P > 0.05$).

Table 1 Baseline Characteristics of mHCC Patients in the Training and Validation Cohort

Variable	Training Cohort (n=193)			Validation Cohort (n=80)			*P* value*
	MVI (+)	MVI (-)	*P* value	MVI (+)	MVI (-)	*P* value	1.000
Age (years)[a]	56.7 ± 11.11	58.5 ± 10.59	0.248	56.6 ± 11.53	57.9 ± 11.21	0.611	0.843
Gender			0.189			0.341	0.117
Male	85 (85.0%)	85 (91.4%)		41 (97.6%)	35 (92.1%)		
Female	15 (15.0%)	8 (8.6%)		1 (2.4%)	3 (7.9%)		
Etiology of liver disease			0.096			0.290	0.524
Hepatitis B virus	87 (87.0%)	89 (95.7%)		36 (85.7%)	36 (94.7%)		
Hepatitis C virus	2 (2.0%)	1 (1.1%)		2 (4.8%)	0 (0.0%)		
None or other	11 (11.0%)	3 (3.2%)		4 (9.5%)	2 (5.3%)		
Edmondson-Steiner grade			0.001			0.020	0.154
I-II	31 (31.0%)	52 (55.9%)		10 (23.8%)			
III-IV	69 (69.0%)	41 (44.1%)		32 (76.2%)	19 (50.0%)		
Liver cirrhosis (P)			0.546		19 (50.0%)	0.216	0.397
Presence	63 (63.0%)	63 (67.7%)		27 (64.3%)	30 (78.9%)		
Absence	37 (37.0%)	30 (32.3%)		15 (35.7%)	8 (21.1%)		
Satellite nodule (P)			0.006			0.436	1.000
Presence	13 (13.0%)	2 (2.2%)		5 (11.9%)	2 (5.3%)		
Absence	87 (87.0%)	91 (97.8%)		37 (88.1%)	36 (94.7%)		
Tumor number (I)[b]	2.0 (2.0, 2.0)	2.0 (2.0, 2.0)	0.815	2.0 (2.0, 2.0)	2.0 (2.0, 2.0)	0.286	0.386
LTD (cm) (I)[a]	5.1 ± 2.86	3.5 ± 1.59	< 0.001	5.0 ± 2.05	3.50 ± 1.71	0.001	0.958
TTD (cm) (I)[a]	7.9 ± 3.67	5.5 ± 2.45	< 0.001	7.5 ± 2.61	5.5 ± 2.38	0.001	0.642
HBV-DNA load			0.215			1.000	0.886
> 10^4 IU/mL	36 (36.0%)	25 (26.9%)		13 (31.0%)	11 (28.9%)		
≤ 10^4 IU/mL	64 (64.0%)	68 (73.1%)		29 (69.0%)	27 (71.1%)		
Serum AFP			0.001			0.144	0.671
< 20 ng/mL	34 (34.0%)	46 (49.5%)		11 (26.2%)	18 (47.4%)		
20–400 ng/mL	28 (28.0%)	33 (35.5%)		19 (45.2%)	12 (31.6%)		
> 400 ng/mL	38 (38.0%)	14 (15.1%)		12 (28.6%)	8 (21.1%)		
TBIL			0.817			0.505	0.671
≤ 20.4 μmol/L	89 (89.0%)	84 (90.3%)		38 (90.5%)	32 (84.2%)		
> 20.4 μmol/L	11 (11.0%)	9 (9.7%)		4 (9.5%)	6 (15.8%)		
DBIL			1.000			0.774	0.737
≤ 6.8 μmol/L	80 (80.0%)	75 (80.6%)		34 (81.0%)	32 (84.2%)		
> 6.8 μmol/L	20 (20.0%)	18 (19.4%)		8 (19.0%)	6 (15.8%)		
TP			0.870			0.349	0.237
≤ 65 g/L	25 (25.0%)	25 (26.9%)		12 (28.6%)	15 (39.5%)		
> 65 g/L	75 (75.0%)	68 (73.1%)		30 (71.4%)	23 (60.5%)		
ALB			0.741			1.000	1.000
≤ 35 g/L	4 (4.0%)	5 (5.4%)		2 (4.8%)	2 (5.3%)		
> 35 g/L	96 (96.0%)	88 (94.6%)		40 (95.2%)	36 (94.7%)		
ALT			0.057			0.596	0.874
> 50 U/L	28 (29.0%)	15 (16.1%)		10 (23.8%)	7 (18.4%)		
≤ 50 U/L	72 (71.0%)	78 (83.9%)		32 (76.2%)	31 (81.6%)		
AST			0.016			0.132	1.000
> 40 U/L	35 (35.0%)	18 (19.4%)		15 (35.7%)	7 (18.4%)		
≤ 40 U/L	65 (65.0%)	75 (80.6%)		27 (64.3%)	31 (81.6%)		
AKP			0.486			1.000	0.651
> 125 U/L	12 (12.0%)	8 (8.6%)		3 (7.1%)	3 (7.9%)		
≤ 125 U/L	88 (88.0%)	85 (91.4%)		39 (92.9%)	35 (92.1%)		

(*Continued*)

Table 1 (Continued).

Variable	Training Cohort (n=193)			Validation Cohort (n=80)			*P* value*
	MVI (+)	MVI (-)	*P* value	MVI (+)	MVI (-)	*P* value	1.000
GGT			0.564			0.125	0.791
> 60 U/L	49 (49.0%)	41 (44.1%)		24 (57.1%)	15 (39.5%)		
≤ 60 U/L	51 (51.0%)	52 (55.9%)		18 (42.9%)	23 (60.5%)		
TBA			0.379			0.350	0.417
> 10 μmol/L	37 (37.0%)	41 (44.1%)		17 (40.5%)	11 (28.9%)		
≤ 10 μmol/L	63 (63.0%)	52 (55.9%)		25 (59.5%)	27 (71.1%)		
PLT			0.349			0.535	0.723
≤ 100◊10^9/L	15 (15.0%)	19 (20.4%)		5 (11.9%)	7 (18.4%)		
> 100◊10^9/L	85 (85.0%)	74 (79.6%)		37 (88.1%)	31 (81.6%)		
PT			1.000			0.664	0.267
> 13s	10 (10.0%)	10 (10.8%)		2 (4.8%)	3 (7.9%)		
≤ 13s	90 (90.0%)	83 (89.2%)		40 (95.2%)	35 (92.1%)		

Notes: Unless otherwise indicated, data are the number of patients, with the percentage in parentheses. *P value for the training cohort and validation cohort. [a]Data are presented as mean ± standard deviation. [b]Data are presented as median (interquartile range). (P): Identified with postoperative pathological examination. (I): Identified with preoperative MRI imaging.

Abbreviations: MVI, microvascular invasion; LTD, the largest tumor diameter; TTD, total tumor diameter; AFP, α-fetoprotein; TBIL, total bilirubin; DBIL, direct bilirubin; TP, total protein; ALB, albumin; ALT, alanine aminotransferase; AST, aspartate aminotransferase; AKP, alkaline phosphatase; GGT, γ-glutamyltranspetidase; TBA, total bile acid; PLT, platelet; PT, prothrombin time.

MR Imaging Characteristics

The MR imaging characteristics of the patients in two cohorts are shown in Table 2. Both qualitative and quantitative features showed moderate to excellent inter-reader agreement, with kappa values ranging from 0.709 to 0.885 and intraclass correlation values ranging from 0.959 to 0.972 (Supplementary Table 2). In the training cohort, mHCC patients with MVI-positive showed satellite nodule ($P < 0.001$), hemorrhage in mass ($P = 0.005$), mosaic architecture ($P < 0.001$), non-smooth tumor margin ($P = 0.004$) more frequently than those with MVI-negative. The TTD values of mHCC patients with MVI-positive were higher than those lacking MVI ($P < 0.001$). The peritumoral enhancement and increased RLSD values were also observed more frequently in MVI-positive groups, though the P value did not reach a statistical significance ($P = 0.052$ and 0.079, respectively).

Table 2 MR Features of mHCC Patients in the Training and Validation Cohort

Variable	Training Cohort (n=193)			Validation Cohort (n=80)			*P* value*
	MVI (+)	MVI (-)	*P* value	MVI (+)	MVI (-)	*P* value	1.000
Tumor number > 2	14 (14.0%)	14 (15.1%)	0.841	5 (11.9%)	8 (21.1%)	0.366	0.853
Liver cirrhosis			0.146			0.641	0.224
Presence	51 (51.0%)	58 (62.4%)		26 (61.9%)	26 (68.4%)		
Absence	49 (49.0%)	35 (37.6%)		16 (38.1%)	12 (31.6%)		
Satellite nodule			< 0.001			0.678	0.506
Presence	20 (20.0%)	1 (1.1%)		4 (9.5%)	2 (5.3%)		
Absence	80 (80.0%)	92 (98.7%)		38 (90.5%)	36 (94.7%)		
Hemorrhage in mass			0.005			0.152	0.237
Presence	34 (34.0%)	15 (16.1%)		17 (40.5%)	9 (23.7%)		
Absence	66 (66.0%)	78 (83.9%)		25 (59.5%)	29 (76.3%)		
Fat in mass			0.066			0.816	0.103
Presence	19 (19.0%)	29 (31.2%)		14 (33.3%)	14 (36.8%)		
Absence	81 (81.0%)	64 (68.8%)		28 (66.7%)	24 (63.2%)		

(*Continued*)

Table 2 (Continued).

Variable	Training Cohort (n=193)			Validation Cohort (n=80)			*P* value*
	MVI (+)	MVI (-)	*P* value	MVI (+)	MVI (-)	*P* value	1.000
Arterial rim enhancement			0.221			0.200	0.287
Presence	12 (12.0%)	6 (6.5%)		8 (19.0%)	3 (7.9%)		
Absence	88 (88.0%)	87 (93.5%)		34 (81.0%)	35 (92.1%)		
Incomplete or absent radiological capsule			0.196			0.022	0.421
Presence	40 (40.0%)	46 (49.5%)		11 (26.2%)	20 (52.6%)		
Absence	60 (60.0%)	47 (50.5%)		31 (73.8%)	18 (47.4%)		
Peritumoral enhancement			0.052			0.329	0.332
Presence	43 (43.0%)	27 (29.0%)		15 (35.7%)	9 (23.7%)		
Absence	57 (57.0%)	66 (71.0%)		27 (64.3%)	29 (76.3%)		
Mosaic architecture			< 0.001			0.073	0.507
Presence	62 (62.0%)	29 (31.2%)		22 (52.4%)	12 (31.6%)		
Absence	38 (38.0%)	64 (68.8%)		20 (47.6%)	26 (68.4%)		
Nodule in nodule architecture			1.000			0.495	1.000
Presence	3 (3.0%)	3 (3.2%)		2 (4.8%)	0 (0.0%)		
Absence	97 (97.0%)	90 (96.8%)		40 (95.2%)	38 (100.0%)		
Non-smooth tumor margin			0.004			0.108	0.640
Presence	84 (84.0%)	61 (65.6%)		30 (71.4%)	33 (86.8%)		
Absence	16 (16.0%)	32 (34.4%)		12 (28.6%)	5 (13.2%)		
Atypical enhancement pattern			0.483			0.012	0.871
Presence	19 (19.0%)	22 (23.7%)		13 (31.0%)	3 (7.9%)		
Absence	81 (81.0%)	71 (76.3%)		29 (69.0%)	35 (92.1%)		
TTD (cm)[a]	7.9 ± 3.67	5.5 ± 2.45	< 0.001	7.5 ± 2.61	5.5 ±2.38	0.001	0.642
RLSD (cm)[a]	2.8 ± 1.88	2.4 ± 1.42	0.079	3.1 ± 2.40	2.8 ± 1.35	0.430	0.167

Notes: Unless otherwise indicated, data are the number of patients, with the percentage in parentheses. *P value for the training cohort and validation cohort. [a]Data are presented as mean ± standard deviation.

Abbreviations: MVI, microvascular invasion; TTD, total tumor diameter; RLSD, the ratio of the largest to the smallest tumor diameter.

Univariable and Multivariable Analysis

The results of univariable and multivariable analysis are shown in Table 3. In the univariable analysis, HBV infection, serum AFP > 400 ng/mL, ALT > 50 U/L, AST > 40 U/L, satellite nodule, hemorrhage in mass, fat in mass, peritumoral enhancement, mosaic architecture, non-smooth tumor margin, LTD, TTD and RLSD were predictors of MVI. The multivariable logistic regression revealed that serum AFP > 400 ng/mL (OR, 3.038, 95% CI, 1.273–7.249, $P = 0.012$), satellite nodule (OR, 12.979, 95% CI, 1.396–120.651, $P = 0.024$), mosaic architecture (OR, 2.052, 95% CI, 1.003–4.198, $P = 0.049$) and TTD (OR, 1.230, 95% CI, 1.064–1.423, $P = 0.005$) were independent risk factors, whereas fat in mass (OR, 0.298, 95% CI, 0.130–0.683, $P = 0.004$) was an independent protective factor of MVI in mHCC.

Development and Validation of Risk Score

A risk score system was developed with the independent predictors of MVI (Table 3). In this study, the 4-cm increase in TTD was defined as a risk score of 1. By rounding the quotient of the regression coefficients divided by the regression coefficient for 4-cm increase (0.207◊4), the regression coefficients for the predictors were converted into integer risk scores, which ranged from 0 to 10 in this study (Table 4). In the training cohort, the risk score showed good discrimination performance with an apparent C-index of 0.777 (95% CI, 0.712–0.841). The optimism-corrected C-index was 0.752. In the validation cohort, the risk score demonstrated an apparent C-index of 0.758 (95% CI, 0.654–0.863) and the corrected C-index was 0.688. The calibration curves showed good calibration between the predicted and actual probability of MVI in both training and validation cohort (Figure 2). The decision curve of the risk score is demonstrated in Supplementary Figure 2.

Table 3 Univariable and Multivariable Analysis of MVI in the Training Cohort

Variable	Univariate Analysis		Multivariate Analysis		
	OR (95% CI)	*P* value	OR (95% CI)	*P* value	Regression Coefficient
Male	0.533 (0.215–1.324)	0.175			
Age	0.985 (0.959–1.011)	0.247			
Etiology of liver disease		0.123			
None or other	1				
Hepatitis B virus	0.267 (0.072–0.998)	0.048			
Hepatitis C virus	0.545 (0.036–8.270)	0.662			
HBV-DNA load > 10^4 IU/mL	1.530 (0.828–2.827)	0.175			
Serum AFP		0.002		0.043	
< 20 ng/mL	1		1		
20–400 ng/mL	1.148 (0.587–2.245)	0.687	1.363 (0.631–2.944)	0.430	
> 400 ng/mL	3.672 (1.724–7.823)	0.001	3.038 (1.273–7.249)	0.012*	1.111
TBIL > 20.4 μmol/L	1.154 (0.455–2.924)	0.763			
DBIL > 6.8 μmol/L	1.042 (0.512–2.120)	0.910			
TP ≤ 65 g/L	0.907 (0.476–1.727)	0.766			
ALB ≤ 35 g/L	0.733 (0.191–2.818)	0.652			
ALT > 50 U/L	2.022 (1.000–4.089)	0.050			
AST > 40 U/L	2.244 (1.161–4.334)	0.016			
AKP > 125 U/L	1.449 (0.564–3.720)	0.441			
GGT > 60 U/L	1.219 (0.691–2.148)	0.494			
TBA > 10 μmol/L	0.745 (0.419–1.326)	0.317			
PLT ≤ 100◊10^9/L	0.687 (0.326–1.448)	0.324			
PT > 13s	0.922 (0.365–2.328)	0.864			
Tumor number > 2	0.919 (0.412–2.047)	0.835			
Liver cirrhosis	0.628 (0.354–1.115)	0.112			
Satellite nodule	23.000 (3.019–175.228)	0.002	12.979 (1.396–120.651)	0.024*	2.563
Hemorrhage in mass	2.679 (1.343–5.342)	0.005			
Fat in mass	0.518 (0.266–1.006)	0.052	0.298 (0.130–0.683)	0.004*	−1.210
Arterial rim enhancement	1.977 (0.710–5.504)	0.192			
Incomplete or absent capsule	0.681 (0.385–1.205)	0.187			
Peritumoral enhancement	1.844 (1.014–3.352)	0.045			
Mosaic architecture	3.601 (1.984–6.537)	< 0.001	2.052 (1.003–4.198)	0.049*	0.719
Nodule in nodule architecture	0.928 (0.183–4.716)	0.928			
Non-smooth tumor margin	2.754 (1.389–5.462)	0.004			
Atypical enhancement pattern	0.757 (0.379–1.612)	0.430			
LTD	1.502 (1.251–1.802)	< 0.001			
TTD	1.326 (1.172–1.500)	< 0.001	1.230 (1.064–1.423)	0.005*	0.207
RLSD	1.170 (0.978–1.399)	0.087			

Notes: *Serum AFP > 400 ng/mL, satellite nodule, fat in mass, mosaic architecture and TTD were independent significant factors in multivariate analyses.
Abbreviations: OR, odds ratio; CI, confidence interval; MVI, microvascular invasion; AFP, α-fetoprotein; TBIL, total bilirubin; DBIL, direct bilirubin; TP, total protein; ALB, albumin; ALT, alanine aminotransferase; AST, aspartate aminotransferase; AKP, alkaline phosphatase; GGT, γ-glutamyltranspetidase; TBA, total bile acid; PLT, platelet; PT, prothrombin time; LTD, largest tumor diameter; TTD, total tumor diameter; RLSD, the ratio of the largest to the smallest tumor diameter.

MVI Risk Score-Based Prognostic Stratification

The cut-off value of the risk score to identify MVI was 5 points, which showed a specificity of 100%. Patients with the risk score <5 was considered the low-risk group and those with the risk score ≥5 was considered the high-risk group (Figures 3 and 4).

When stratified based on the risk score, in the training cohort, the 1-year, 2-year RFS rates of high-risk patients were 43.5% and 26.4% and the 1-year, 2-year RFS rates of low-risk patients were 75.1% and 61.2%. In the validation cohort, the 1-year, 2-year RFS rates of high-risk patients were 58.3% and 25.0% and the 1-year, 2-year RFS rates of low-risk

Table 4 Risk Score for Factors Associated with MVI of Multinodular HCC

Parameter	Score
AFP	
≤ 400 ng/mL	0
> 400 ng/mL	1
Satellite nodule (I)	
Absence	0
Presence	3
Fat in mass	
Presence	0
Absence	1
Mosaic architecture	
Absence	0
Presence	1
TTD	
≤ 4 cm	0
4–8 cm	1
8–12 cm	2
12–16 cm	3
≥ 16 cm	4

Note: (I) means the satellite nodule on MR imaging.
Abbreviations: AFP, α-fetoprotein; TTD, total tumor diameter.

patients were 73.2% and 46.5%. Kaplan–Meier survival curve based on the risk score are plotted in Figure 5. Patients in the low-risk group showed a significantly better prognosis than those in the high-risk group ($P < 0.001$ for the training cohort and $P = 0.038$ for the validation cohort).

Discussion

The present study demonstrated that serum AFP > 400 ng/mL, presence of satellite nodule, mosaic architecture and increased TTD were independent predictors of MVI, while fat in mass was an independent protective factor of MVI in mHCC. Moreover, a simple and practical risk score system with good discrimination, calibration performance and clinical usefulness was constructed and verified. Through the risk score system, patients with resectable mHCC could be preoperatively stratified into two groups with low/high risks of MVI, which is helpful to the prognosis evaluation and individualized treatment of patients.

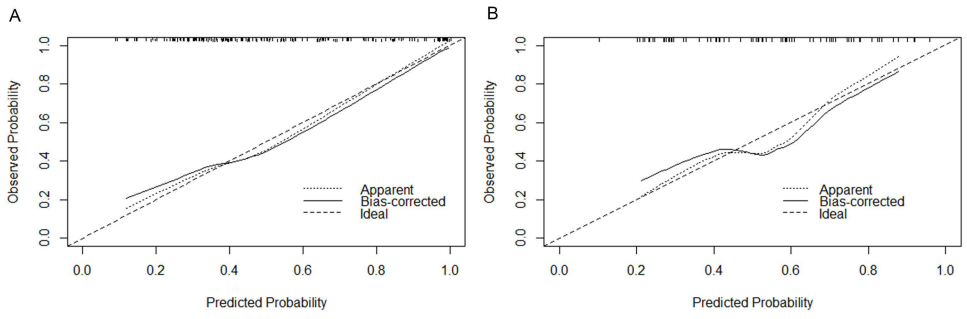

Figure 2 The calibration curve compared predicted and observed probability of microvascular invasion in the (**A**) training cohort and (**B**) validation cohort.

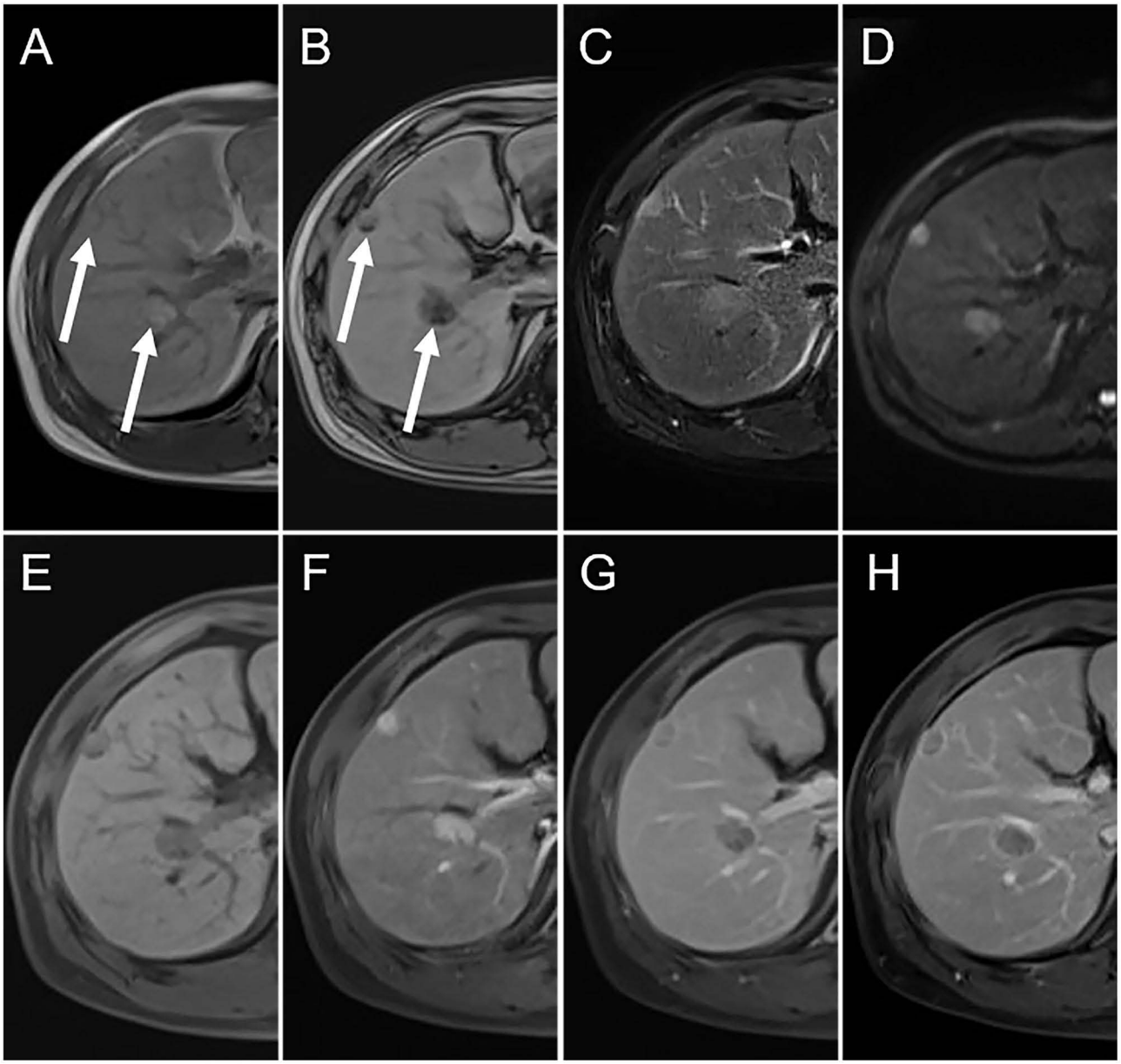

Figure 3 47-year-old man without pathological microvascular invasion. The serum α-fetoprotein was < 400 ng/mL. The Axial contrast-enhanced MR demonstrated two HCC lesions in the right liver section with the total diameter of 3.7 cm. Both lesions contained fat (**A** and **B**, white arrows) and demonstrated hyperintense on T2-weighted image (**C**), diffusion-weighted image (**D**) and hypointense on T1-weighted image (**E**). After the injection of contrast agent, both lesions showed typical enhancement pattern with enhancement on the arterial phase (**F**) and washout on the portal phase (**G**) and delayed phase (**H**). Both lesions showed compete radiological capsule. Risk score value of 0 score categorized the patient into low-risk group. After the surgery, no recurrence was observed and the recurrence-free survival was 36 months.

MVI is widely accepted as a predominant factor associated with decreased RFS and OS after surgery.[11] In single-nodular HCC, MVI has been proved as the prominent factor affecting postoperative prognosis and the risk factors of MVI have also been widely studied. However, the impact of MVI on the postoperative prognosis and the clinicoradiological risk factors for MVI in mHCC patients have been rarely investigated. In our cohort, mHCC patients with histological MVI showed significantly decreased 1- and 2-year RFS rates than those without MVI (The 1- and 2-year RFS rates: 57.7%, 29.9% in patients with MVI-positive and 74.0%, 45.6% in patients with MVI-negative), suggesting the importance of status of MVI in postoperative prognosis of patients with resectable mHCC. In previous studies involving mHCC, researchers only evaluated the radiological features of the largest tumor while ignored the feature of the other HCC lesions, which might lead to the underestimation of MVI status.[17,25,26] Due to the substantial intertumoral

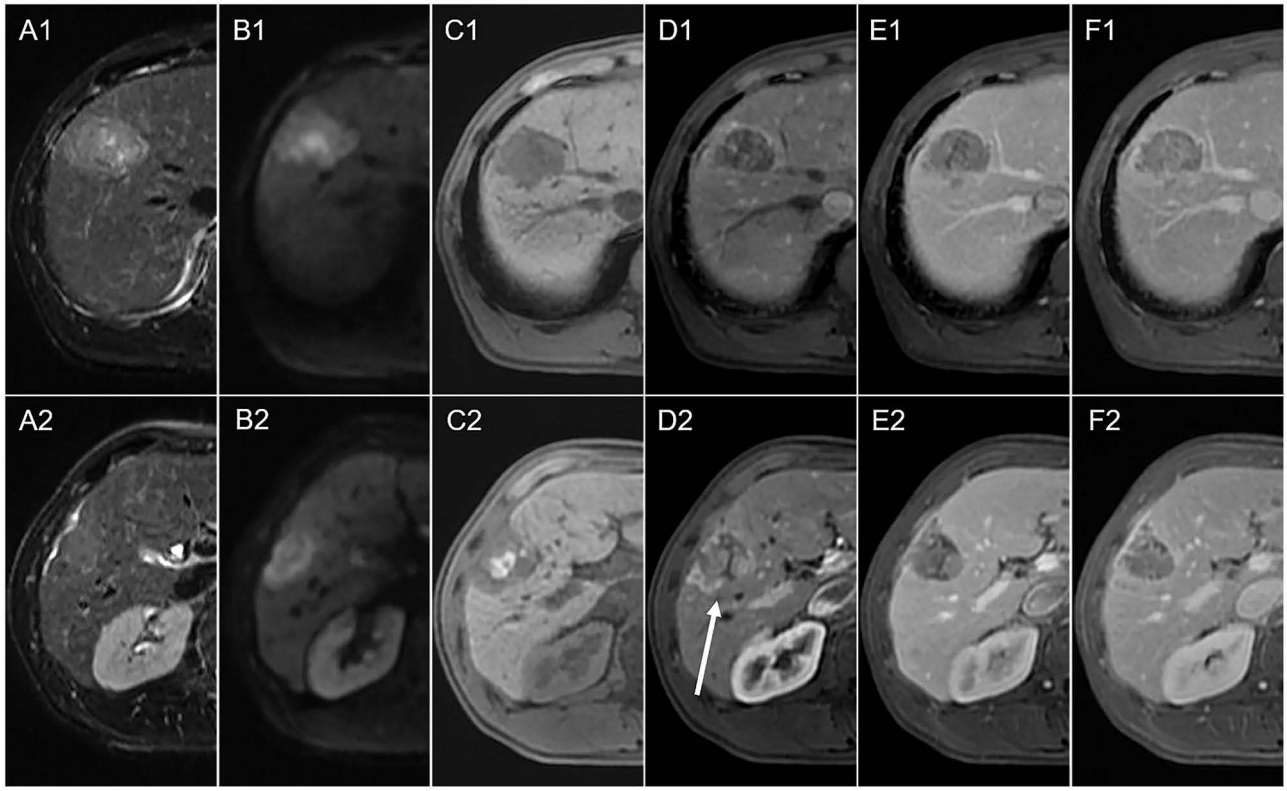

Figure 4 56-year-old man with pathological microvascular invasion. The serum α-fetoprotein was > 400 ng/mL. Axial contrast-enhanced MR demonstrated two HCC lesions in the right liver section with the total diameter of 9.5 cm. Both lesions showed hyperintense on T2-weighted image (**A1** and **A2**) and diffusion-weighted image (**B1** and **B2**) and hypointense on T1-weighted image (**C1** and **C2**). Both lesions showed typical enhancement pattern with enhancement on the arterial phase (**D1** and **D2**) and washout on the portal phase (**E1** and **E2**) and delayed phase (**F1** and **F2**). The smaller lesion showed hemorrhage in mass (**C2**) and mosaic architecture (**D2**, arrow). The tumor emboli were found in the specimen sampled at the junction of the smaller tumor (**A2**–**F2**) and adjacent liver tissues. Risk score value of 5 categorized the patient into high-risk group. After surgery, recurrence was observed and the recurrence-free survival was 9 months.

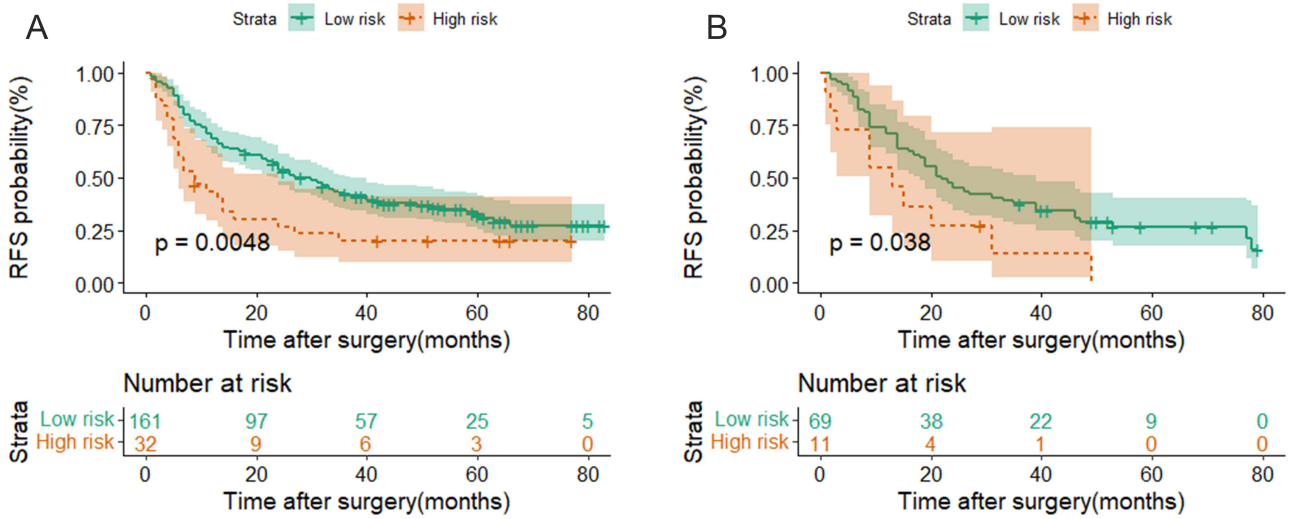

Figure 5 MVI Risk Score-based Prognostic Stratification. Graphs showed that multinodular HCC patients in the low-risk groups had significantly shorter RFS than those in the high-risk group in the (**A**) training cohort and (**B**) validation cohort (Log rank test, both $P < 0.05$).
Abbreviations: MVI, Microvascular Invasion; RFS, Recurrence-free Survival.

heterogeneity in mHCC, some small tumors may manifest with aggressive biological behavior and contribute to the presence of MVI.[27–30] Therefore, in this study, the imaging characteristics of all tumors were included and analyzed to determine the status of MVI in patients with mHCC.

This study showed mosaic architecture was an independent risk factor of MVI in mHCC patients, which was in line with a previous result reported by Chen et al.[17] It refers to the presence of multiple internal tumor nodules within the tumor separated by fibrous septations and areas of hemorrhage, necrosis, and occasionally fatty metamorphosis.[31] The various nodules represent clonal expansion of aberrant cells at different phases, potentially ranging from dysplasia to poorly differentiated malignancy, which may explain the association with MVI. Additionally, mosaic architecture, as a common feature of advanced HCC, represents the high intratumoral heterogeneity of multiple HCC lesions, indicating a high risk of MVI. TTD is the total tumor diameter of mHCC, reflecting the tumor burden more accurately than tumor diameter or number alone. The increase in TTD suggests a high tumor burden in patients with mHCC, which is usually correlated with an increased probability of MVI.[16]

Previously, a number of studies suggested serum AFP > 400 ng/mL was associated with more aggressive biological behavior of tumor and therefore a higher likelihood of MVI formation, which was consistent with our result.[16,32] As for satellite nodule, it pathologically refers to the macroscopic or microscopic tumor cell nests located around but separated from the main tumor.[12] Directly derived from MVI, it represents intrahepatic metastases within the venous drainage area around the main tumor.[31,32] Since some visible satellite nodules could be detected on MR imaging, this feature was included in the model and showed a high predictive value.

In this study, fat in mass was an independent protective factor of MVI of patients with mHCC, which has never been reported in single-nodular HCC. Due to the fat accumulation within hepatocytes during the early phase of hepatocarcinogenesis, this feature was considered a characteristic of early HCC with less aggressive biological behavior.[31] In addition, in patients with mHCC, fat in mass may represent a high likelihood of multicentric origin of multiple lesions, which was reported a better prognosis than intrahepatic metastases.[33,34] As a result, mHCC patients with this imaging feature may be less likely to develop MVI.

Considering the great impact of MVI on postsurgical recurrence in patients with mHCC, we established and validated a clinically applicable prediction model by combining the abovementioned clinicoradiological variables, which was presented as a risk score. This simple risk score system could accurately and reliably predict the status MVI among patients with mHCC with the C-index of 0.777 and 0.758 in the training and validation cohort, respectively. Previously, most studies have focused on the construction of single clinical factors-based prognostic risk models for resectable mHCC.[16] By contrast, in this study, both clinical and radiological factors were included in the risk score, providing more information about the biological characteristics of tumors and more accurately predicting the status of MVI. Additionally, these comprehensive variables in our study enable to normalized acquisition, making the risk score highly feasible. Based on the risk scoring system, patients with mHCC were preoperatively stratified into two groups. Patients in the high-risk group showed significantly decreased 1- and 2-year RFS rates compared with those in the low-risk group. Therefore, when making a personalized therapeutic regime, whether a surgical resection should be further considered in mHCC patients at a high predicted risk of MVI, since targeted therapy based on the molecular profile of the original tumor might be a better option.[28] However, for those at a low predicted risk of MVI, a radical liver resection may be a preferred treatment option.

The current study had several limitations. First, we retrospectively selected mHCC patients based on imaging diagnosis, and some patients with undiscernible HCC on MRI might have been excluded from this study, which led to selection bias. Second, an external validation is lacking in this study. Finally, most patients (90.8%) in this study had HBV-related chronic liver disease. Therefore, when interpreting the results, the underlying etiology of the population should be considered.

In conclusion, serum AFP > 400 ng/mL, presence of satellite nodule, mosaic architecture and increased TTD were independent risk factors of MVI while fat in mass was an independent protective factor in patients with resectable mHCC. A simple and practical risk score preoperatively enabled an accurate risk stratification, which is helpful to the prognosis evaluation and individualized treatment of mHCC patients.

Abbreviations

mHCC, multinodular hepatocellular carcinoma; MVI, microvascular invasion; AFP, α-fetoprotein; TTD, total tumor diameter; MR, magnetic resonance imaging; HBV-DNA, HBV deoxyribonucleic acid; LTD, largest tumor diameter; RLSD, the ratio of the largest to the smallest tumor diameter; RFS, recurrence-free survival.

Author Contributions

All authors made a significant contribution to the work reported, whether that is in the conception, study design, execution, acquisition of data, analysis and interpretation, or in all these areas; took part in drafting, revising or critically reviewing the article; gave final approval of the version to be published; have agreed on the journal to which the article has been submitted; and agree to be accountable for all aspects of the work.

Funding

This study has received funding by Shanghai Municipal Health Commission (grant number 202240152), the National Natural Science Foundation of China (grant number 82171897), Shanghai Municipal Key Clinical Specialty (grant number shslczdzk03202), Clinical Research Plan of SHDC (grant number SHDC2020CR1029B), China National Key R&D Program (grant number 2022YFC2401605), Scientific Research Development Plan of SHDC and UNITED IMAGING (grant number SKLY2022CRT201), "Science and Technology Innovation Action Plan" Star Cultivation (Sailing Program) (grant number 22YF1443600) and Youth Foundation of Shanghai Municipal Health Commission (20204Y0346).

Disclosure

The authors report no conflicts of interest in this work.

References

1. Kudo M, Izumi N, Ichida T, et al. Report of the 19th follow-up survey of primary liver cancer in Japan. *Hepatol Res*. 2016;5(46):372–390. doi:10.1111/hepr.12697
2. Cao L, Cheng H, Jiang Q, Li H, Wu Z. APEX1 is a novel diagnostic and prognostic biomarker for hepatocellular carcinoma. *Aging*. 2020;5(12):4573–4591.
3. Wu Z, Cheng H, Liu J, et al. The oncogenic and diagnostic potential of stanniocalcin 2 in hepatocellular carcinoma. *J Hepatocell Carcinoma*. 2022; Volume 9:141–155. doi:10.2147/JHC.S351882
4. Villanueva A. Hepatocellular Carcinoma. *N Engl J Med*. 2019;15(380):1450–1462. doi:10.1056/NEJMra1713263
5. Hyun MH, Lee YS, Kim JH, et al. Hepatic resection compared to chemoembolization in intermediate- to advanced-stage hepatocellular carcinoma: a meta-analysis of high-quality studies. *Hepatology*. 2018;3(68):977–993. doi:10.1002/hep.29883
6. Yin L, Li H, Li AJ, et al. Partial hepatectomy vs. transcatheter arterial chemoembolization for resectable multiple hepatocellular carcinoma beyond Milan Criteria: a RCT. *J Hepatol*. 2014;1(61):82–88. doi:10.1016/j.jhep.2014.03.012
7. Zaydfudim VM, Vachharajani N, Klintmalm GB, et al. Liver resection and transplantation for patients with hepatocellular carcinoma beyond Milan criteria. *Ann Surg*. 2016;4(264):650–658. doi:10.1097/SLA.0000000000001866
8. Zhong JH, Ke Y, Gong WF, et al. Hepatic resection associated with good survival for selected patients with intermediate and advanced-stage hepatocellular carcinoma. *Ann Surg*. 2014;2(260):329–340. doi:10.1097/SLA.0000000000000236
9. Hong SB, Choi SH, Kim SY, et al. MRI Features for predicting microvascular invasion of hepatocellular carcinoma: a systematic review and meta-analysis. *Liver Cancer*. 2021;2(10):94–106. doi:10.1159/000513704
10. Rodríguez-Perálvarez M, Luong TV, Andreana L, Meyer T, Dhillon AP, Burroughs AK. A systematic review of microvascular invasion in hepatocellular carcinoma: diagnostic and prognostic variability. *Ann Surg Oncol*. 2013;1(20):325–339. doi:10.1245/s10434-012-2513-1
11. Zhang X, Li J, Shen F, Lau WY. Significance of presence of microvascular invasion in specimens obtained after surgical treatment of hepatocellular carcinoma. *J Gastroen Hepatol*. 2018;2(33):347–354. doi:10.1111/jgh.13843
12. Cong W, Bu H, Chen J, et al. Practice guidelines for the pathological diagnosis of primary liver cancer: 2015 update. *World J Gastroentero*. 2016;42(22):9279. doi:10.3748/wjg.v22.i42.9279
13. Li M, Yin Z, Hu B, et al. MR elastography-based shear strain mapping for assessment of microvascular invasion in hepatocellular carcinoma. *Eur Radiol*. 2022;7(32):5024–5032. doi:10.1007/s00330-022-08578-w
14. Lee S, Kim SH, Lee JE, Sinn DH, Park CK. Preoperative gadoxetic acid–enhanced MRI for predicting microvascular invasion in patients with single hepatocellular carcinoma. *J Hepatol*. 2017;3(67):526–534. doi:10.1016/j.jhep.2017.04.024
15. Chandarana H, Robinson E, Hajdu CH, Drozhinin L, Babb JS, Taouli B. Microvascular invasion in hepatocellular carcinoma: is it predictable with pretransplant MRI? *Am J Roentgenol*. 2011;5(196):1083. doi:10.2214/AJR.10.4720
16. Zhao WC, Fan LF, Yang N, Zhang HB, Chen BD, Yang GS. Preoperative predictors of microvascular invasion in multinodular hepatocellular carcinoma. *Eur J Surg Oncol*. 2013;8(39):858–864. doi:10.1016/j.ejso.2013.04.003

17. Chen J, Zhou J, Kuang S, et al. Liver imaging reporting and data system category 5: MRI predictors of microvascular invasion and recurrence after hepatectomy for hepatocellular carcinoma. *AJR Am J Roentgenol*. 2019;4(213):821–830. doi:10.2214/AJR.19.21168
18. Zhang K, Xie SS, Li WC, Ye ZX, Shen ZW, Shen W. Prediction of microvascular invasion in HCC by a scoring model combining Gd-EOB-DTPA MRI and biochemical indicators. *Eur Radiol*. 2022;6(32):4186–4197. doi:10.1007/s00330-021-08502-8
19. Dong S, Wang W, Chen X, et al. Microvascular invasion of small hepatocellular carcinoma can be preoperatively predicted by the 3D quantification of MRI. *Eur Radiol*. 2022;6(32):4198–4209. doi:10.1007/s00330-021-08495-4
20. Chong H, Yang L, Sheng R, et al. Multi-scale and multi-parametric radiomics of gadoxetate disodium–enhanced MRI predicts microvascular invasion and outcome in patients with solitary hepatocellular carcinoma ≤ 5 cm. *Eur Radiol*. 2021;7(31):4824–4838. doi:10.1007/s00330-020-07601-2
21. Goldberg D, Mantero A, Newcomb C, et al. Predicting survival after liver transplantation in patients with hepatocellular carcinoma using the LiTES-HCC score. *J Hepatol*. 2021;6(74):1398–1406. doi:10.1016/j.jhep.2020.12.021
22. Wang S, Tian S, Li Y, et al. Development and validation of a novel scoring system developed from a nomogram to identify malignant pleural effusion. *Ebiomedicine*. 2020;58:102924. doi:10.1016/j.ebiom.2020.102924
23. Kim AY, Sinn DH, Jeong WK, et al. Hepatobiliary MRI as novel selection criteria in liver transplantation for hepatocellular carcinoma. *J Hepatol*. 2018;6(68):1144–1152. doi:10.1016/j.jhep.2018.01.024
24. Roayaie S, Blume IN, Thung SN, et al. A system of classifying microvascular invasion to predict outcome after resection in patients with hepatocellular carcinoma. *Gastroenterology*. 2009;3(137):850–855. doi:10.1053/j.gastro.2009.06.003
25. Banerjee S, Wang DS, Kim HJ, et al. A computed tomography radiogenomic biomarker predicts microvascular invasion and clinical outcomes in hepatocellular carcinoma. *Hepatology*. 2015;3(62):792–800. doi:10.1002/hep.27877
26. Yang L, Gu D, Wei J, et al. A radiomics nomogram for preoperative prediction of microvascular invasion in hepatocellular carcinoma. *Liver Cancer*. 2019;5(8):373–386. doi:10.1159/000494099
27. Lu L, Hsu C, Hsu C, Cheng A. Tumor heterogeneity in hepatocellular carcinoma: facing the challenges. *Liver Cancer*. 2016;2(5):128–138. doi:10.1159/000367754
28. Gao Q, Wang X, Zhou J, Fan J. Multiple carcinogenesis contributes to the heterogeneity of HCC. *Nat Rev Gastro Hepat*. 2015;1(12):13. doi:10.1038/nrgastro.2014.6-c1
29. Xu LX, He MH, Dai ZH, et al. Genomic and transcriptional heterogeneity of multifocal hepatocellular carcinoma. *Ann Oncol*. 2019;6(30):990–997. doi:10.1093/annonc/mdz103
30. Song D, Wang Y, Wang W, et al. Using deep learning to predict microvascular invasion in hepatocellular carcinoma based on dynamic contrast-enhanced MRI combined with clinical parameters. *J Cancer Res Clin*. 2021;12(147):3757–3767. doi:10.1007/s00432-021-03617-3
31. Choi JY, Lee JM, Sirlin CB. CT and MR imaging diagnosis and staging of hepatocellular carcinoma: part I. Development, growth, and spread: key pathologic and imaging aspects. *Radiology*. 2014;3(272):635–654. doi:10.1148/radiol.14132361
32. Mchugh PP, Gilbert J, Vera S, Koch A, Ranjan D, Gedaly R. Alpha-fetoprotein and tumour size are associated with microvascular invasion in explanted livers of patients undergoing transplantation with hepatocellular carcinoma. *HPB*. 2010;1(12):56–61. doi:10.1111/j.1477-2574.2009.00128.x
33. Ajr AJOR. Liver Reporting & Data System (LI-RADS). Available from: www.acr.org/Clinical-Resources/Reporting-and-Data-Systems/LI-RADS. Accessed April 29, 2022.
34. Yang S, Luo Y, Chen M, et al. A systematic review and meta-analysis comparing the prognosis of multicentric occurrence and vs. intrahepatic metastasis in patients with recurrent hepatocellular carcinoma after hepatectomy. *Hpb*. 2017;10(19):835–842. doi:10.1016/j.hpb.2017.06.002